Numerical study of similarity in prototype and model pumped turbines

Z J Li, Z W Wang, H L Bi
Institute of Fluid Machinery and Fluid Engineering, Department of Thermal Engineering, Tsinghua University, Beijing, 100084, China

Email: wzw@mail.tsinghua.edu.cn

Abstract. Similarity study of prototype and model pumped turbines are performed by numerical simulation and the partial discharge case is analysed in detail. It is found out that in the RSI (rotor-stator interaction) region where the flow is convectively accelerated with minor flow separation, a high level of similarity in flow patterns and pressure fluctuation appear with relative pressure fluctuation amplitude of model turbine slightly higher than that of prototype turbine. As for the condition in the runner where the flow is convectively accelerated with severe separation, similarity fades substantially due to different topology of flow separation and vortex formation brought by distinctive Reynolds numbers of the two turbines. In the draft tube where the flow is diffusively decelerated, similarity becomes debilitated owing to different vortex rope formation impacted by Reynolds number. It is noted that the pressure fluctuation amplitude and characteristic frequency of model turbine are larger than those of prototype turbine. The differences in pressure fluctuation characteristics are discussed theoretically through dimensionless Navier-Stokes equation. The above conclusions are all made based on simulation without regard to the penstock response and resonance.

1. Introduction

Prior to the manufacture and operation of prototype turbine, model test has to be made as an estimation of the real unit performance. To better reflect the actual working condition of prototype turbine, flow in the model turbine should be similar to that in the prototype one. Specifically speaking, all the similarity principles should be complied with, including geometric, kinematic, dynamic, initial condition and boundary condition similarity. However, it is never possible in engineering fields to satisfy all the similarity principles with some of which even contradict with each other. Therefore, it is only conceivable to guarantee the similarity of dominant forces. For pumped turbine, Strouhal number and Euler number are required for the similarity of model turbine and prototype one. The equivalence of Reynolds number, however, cannot be satisfied owing to a raised water head model test can barely reach. Failing to meet the equivalence of Reynolds number contributes to the discrimination of certain flow features and performance, which in turn gives rise to deviation in similarity conversion from model turbine to prototype one. The Froude number inequality will also bring about certain scale effect, but its influence is usually considered minor for high head pumped turbines. Only when the connections between the prototype and model are well established, can the model test results be effectively and correctly converted to prototype ones. Many researchers are trying to establish the pressure fluctuation relation between prototype turbine and its scaled model turbine. Bue [1] analyzed the tendencies development of the relative pressure pulsation amplitudes between a model Francis turbine and its geometrically similar prototype from model tests and field measurements, but it turned

out inapplicable to conclude a scale-up relation through the tendency development. Jacob [2] explained the surge instability in a prototype Francis turbine from numerical results of model turbine based on cavitation appliance parameter. A similar method introducing hydro acoustic model was also applied by Alligné [3] in predicting the instability frequency of a Francis prototype turbine based on the measurements and CFD simulation of its reduced scale mode. The predicted instability frequency generally agrees with the prototype measurements. Wu [4] and Liu [5] analyzed the similarity in pressure fluctuation of a Kaplan prototype turbine and its model turbine. Liu argued that there is no similarity law for pressure fluctuation between the Kaplan model and prototype turbines, while Wu claimed identical dominant frequencies except at low frequencies are observed in the two turbines due to the distinction in eddy diffusivity brought by different Reynolds numbers. The influence of Reynolds number, characterizing the viscous effect, can be vital in topological structure of the separated flow and vortex shedding [6, 7, 8]. Thus the Reynolds number effect on the similarity study of model and pump turbine need to be well considered.

Despite the extensive study concerning flow pattern and pressure fluctuation of hydraulic turbine, few studies focus on the mechanism of Reynolds number effect on the similarity of model turbine and prototype turbine. In this paper, numerical simulation of prototype pumped turbine of Xiangshuijian Pumped Storage Power Station is carried out, along with its model turbine. Comparison and analysis have been made on the external characteristics, flow patterns and pressure fluctuations of the two pumped turbines. The possible existent similarity relations are established and discussed based on the numerical calculation and the differences caused by Reynolds number effect are discussed qualitatively by dimensionless Navier-Stokes equation. Gravity is not considered in the simulation since the influence of Froude number is relatively small.

2. Numerical methods

2.1. Computation region

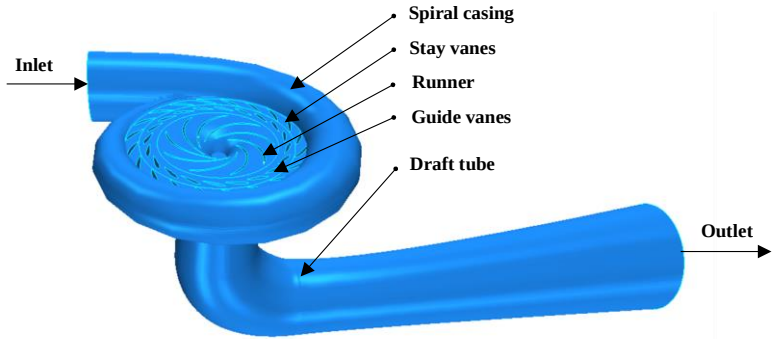

Figure 1. Computation domain of the pumped turbine

The computation domain includes spiral casing, stay vanes, guide vanes, runner and draft tube, as shown in figure 1. The prototype turbine has a runner outlet diameter D_2 of 3.29 m while its scaled model turbine is 0.30 m in runner outlet diameter. The Reynolds number typically used for the pumped turbine is based on the inlet dimension of the spiral casing ($\mathrm{Re}=V_{inlet}D_{inlet}/\upsilon$) and is 1.09×10^6 for the model turbine and 3.04×10^7 for the prototype one. The main geometry data are summarized in Table 1.

2.2. Operating condition and boundary condition

Rotational speed n and discharge Q are normalized by runner diameter D and water head H in Equation. (1). Unit speed n_{11} and unit discharge Q_{11} are derived from Euler number and Strouhal number, the guarantee of which ensures the similarity of prototype turbine and model turbine in

engineering field. Three sets of operating conditions I, II and III in turbine mode are listed in Table 2 for similarity study.

$$n_{11} = \frac{nD}{\sqrt{H}} \qquad Q_{11} = \frac{Q}{D^2\sqrt{H}} \tag{1}$$

Table 1. Pumped turbine geometry

Geometry		Model	Prototype
Runner inlet diameter	D_1(m)	0.49	5.37
Runner outlet diameter	D_2(m)	0.30	3.29
Runner blades	Z	9	9
Stay vanes	Z_S	20	20
Guide vanes	Z_G	`20	20

At the inlet of the spiral casing, a total pressure corresponds to the water head H is specified while at the outlet static pressure zero is prescribed. No-slip boundary condition is imposed on all the solid walls and sliding mesh technique is applied to take into account the rotor stator interaction. The computational solution of steady state simulation of the pumped turbine is employed as an initial condition of the unsteady computation and the time step size is specified such that one runner evolution is divided into 100 time steps, which is considered sufficient to resolve the main flow structure of interest.

Table 2. Pumped turbine operating conditions

Operating conditions		Model			Prototype		
		I	II	III	I	II	III
Head	H(m)	30	30	30	190	190	190
Rotation rate	n(rpm)	1089	1089	1089	250	250	250
Unit speed	n_{11}	59.67	59.67	59.67	59.67	59.67	59.67
Guide vane opening	$\alpha(^\circ)$	32.5	24.5	16	32.5	24.5	16
Flow rate	Q(L/s)	455	370	239	137437	112854	72536
Unit flow rate	Q_{11}	930	764	475	921	761	481

2.3. Grid convergence check

Polyhedral mesh is used in the simulation for being able to improve the overall cell quality and reduce cell number when compared to equivalent tetrahedral meshes. To determine the grid convergence, five sets of computational meshes, shown in Table 3, have been generated for model turbine and prototype turbine, respectively. The influence of mesh numbers on the performance of turbine is shown in figure 2 based on steady simulation adopting *SST* $k-\omega$ turbulence model of operating condition II. Mesh numbers of prototype turbine are set to be larger than those of model turbine to alleviate the deviations caused by different resolution of boundary effects. Considering both the accuracy and computational cost, Mesh Set D is chosen for the numerical simulation of the two turbines.

Table 3. Five sets of computational meshes for model turbine and prototype turbine

Computational meshes		A	B	C	D	E
Model turbine	Mesh number	6.19×10^5	9.46×10^5	1.11×10^6	1.36×10^6	1.63×10^6
	Node number	3.63×10^6	4.16×10^6	5.43×10^6	6.01×10^6	6.33×10^6
Prototype turbine	Mesh number	8.50×10^5	1.20×10^6	1.56×10^6	1.75×10^6	2.16×10^6
	Node number	4.32×10^6	5.90×10^6	6.07×10^6	6.50×10^6	6.90×10^6

The computed efficiency and mass flow of model turbine have been compared with experimental results in figure 3. The simulation results adopting Mesh Set D show good agreement with experimental results, which indicates the reliability of the current numerical method and mesh setting in predicting the external characteristics of the turbines.

2.4. Monitor lines and points

Monitor lines are set to record the velocity distribution of the turbines. As shown in figure 4 and 5, monitor lines d1-d1' is located in the central passage of RSI region, r1-r1', r2-r2' and r3-r3' are set at three different diameters of the runner passage, while t1-t1', t2-t2' and t3-t3' are positioned in the draft tube cone at z/D_2=-0.45, z/D_2=-1.28 and z/D_2=-2.00, respectively. Pressure fluctuations are recorded at three monitor points. P1 and P2 are positioned in the trailing edge of guide vane and leading edge of runner blade, respectively, while P3 is located in the near wall of draft tube at z/D_2=2.00.

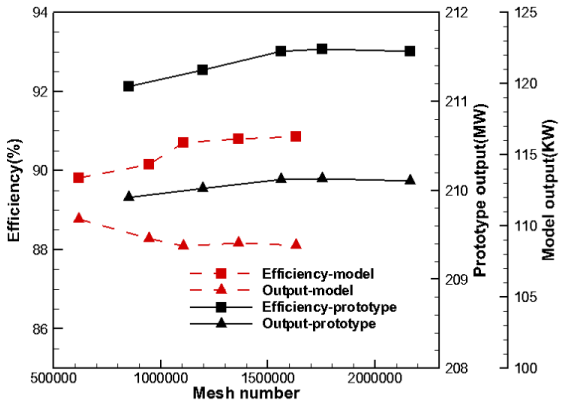

Figure 2. Grid independence on performance of model turbine and prototype turbine

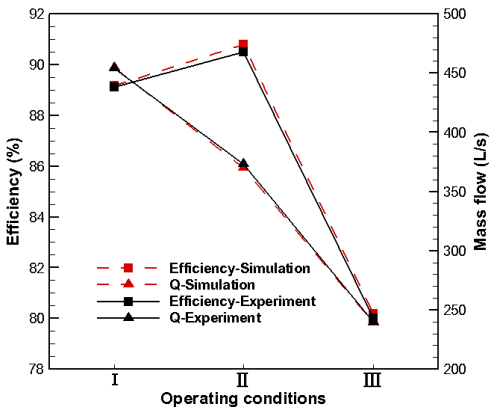

Figure 3. Comparison of simulation and experiment results of model turbine

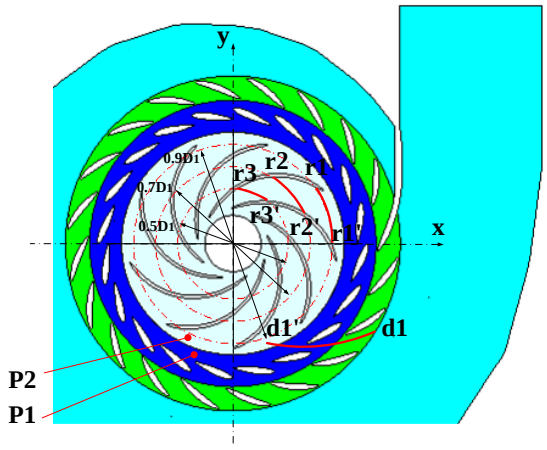

Figure 4. Locations of monitor points and monitor lines at z=0 in the distributor and runner

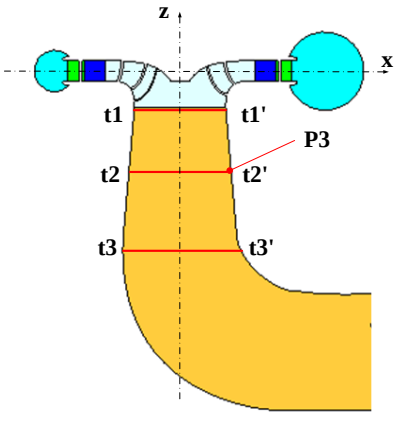

Figure 5. Locations of monitor point and monitor lines in the draft tube

3. Results and Discussion

3.1. Comparison of External Characteristics

The external characteristics of model and prototype turbines are compared in Table 3. Reynolds number signifies the ratio of inertial force and viscous force, indicating greater viscous force in model

turbine. As stronger viscous effect brings about greater energy loss, the efficiency of model turbine is smaller than that of prototype turbine.

Table 4. External characteristics comparison of model turbine and prototype turbine

Operating conditions	**I**		**II**		**III**	
	Prototype	Model	Prototype	Model	Prototype	Model
M (Nm)	8.82×10^6	1.05×10^2	7.47×10^6	8.67×10^2	4.30×10^6	4.94×10^2
P (kW)	2.55×10^5	1.34×10^2	2.10×10^5	1.08×10^2	1.35×10^5	0.70×10^2
η (%)	90.27	89.16	93.08	90.79	83.38	80.19

3.2. Flow Pattern and Pressure Fluctuation of partial discharge condition in the RSI Region

In the present study, partial discharge Condition III, is chosen as an example in discussing the flow patterns and pressure fluctuation characteristics, while lack of space forbids further discussion and explanation of Condition I and II. The dimensionless velocity (defined as $\mathbf{V}^* = \mathbf{V}/\mathbf{V}_{inlet}$) field in the mid-height of the distributor is shown in figure 5. It can be seen that in the RSI region where Strouhal number dominates, the flows in the two turbines are convectively accelerated with minor separation, showing a rather similar flow pattern.

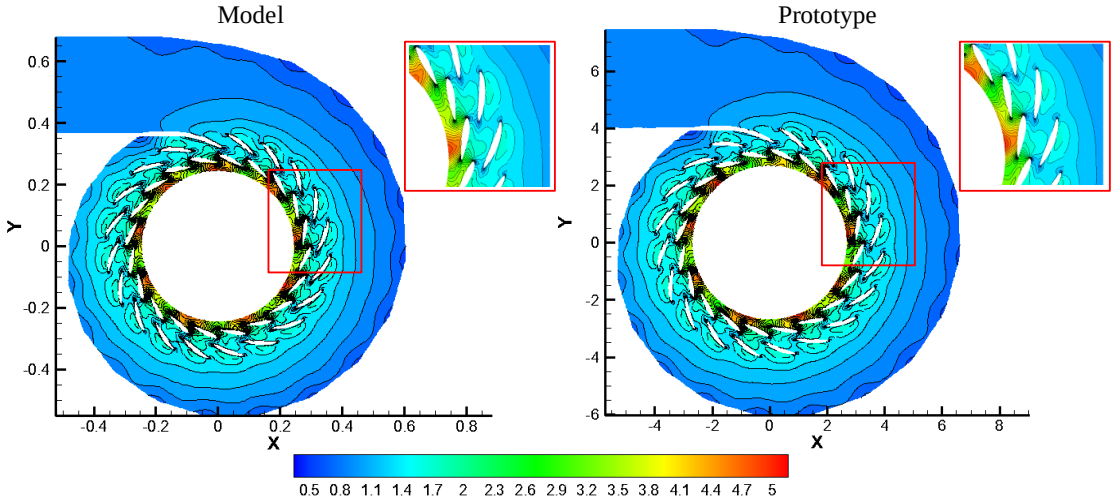

Figure 5. Comparison of dimensionless velocity field at mid-height of the distributor

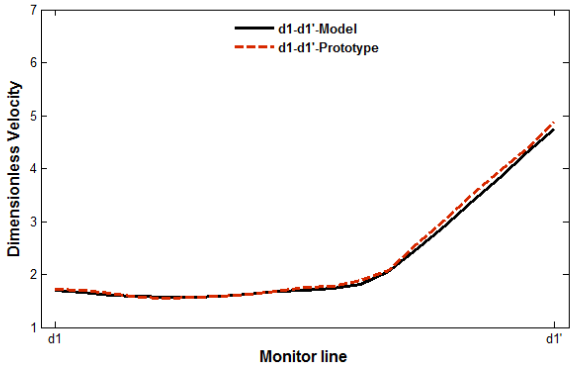

Figure 6. Dimensionless velocity at monitor line d1-d1' in the RSI region

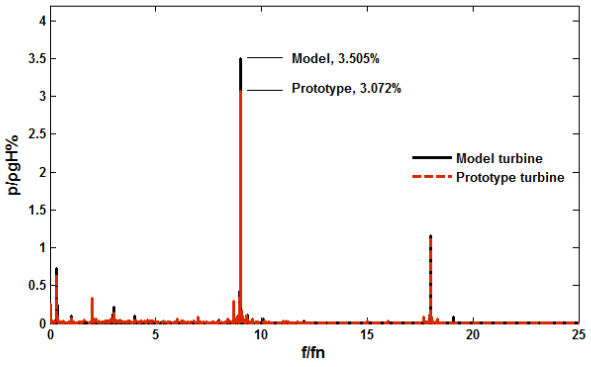

Figure 7. Pressure fluctuation spectrum at monitor point P1

To be more specific on the flow pattern in the rotor-stator interaction (RSI) region, dimensionless velocity at monitor line d1-d1' is depicted in figure 6. It can be seen that the dimensionless velocities

along the monitor lines of the two turbines are nearly identical, again indicating a high level of similarity in flow pattern of the model and prototype turbines.

In order to test the pressure fluctuation condition in RSI region, monitor points P1 and P2 are set at the trailing edge of the guide vane and leading edge of the runner blade, respectively. Without regard to the response of penstock and resonance of water body and structure, the pressure fluctuations in the distributor and runner caused by RSI show certain similarity, as shown in figure 7 and figure 11. As the equality of Strouhal number is fully satisfied, the blade passing frequency 9fn of P1 and guide vane passing frequency 20fn of P2 are exactly identical for the two turbines. However, it is noted that the pressure fluctuation amplitude of model turbine is slightly higher than that of prototype turbine. Similar findings can also be seen in the rotor-stator interaction study from Yan [9] and pressure pulsation comparison between model test and field measurements from Bue [1]. With introduction of dimensionless Navier-Stokes equation, such deviation in relative pressure fluctuation amplitude can be theoretically explained as follows:

With Characteristic velocity V，Characteristic length L，Characteristic pressure p_0，Characteristic mass g，Characteristic time $1/\omega$，Navier-Stokes equation can be transformed into a dimensionless form as below:

$$St\frac{\partial \mathbf{V}^*}{\partial t^*} + \mathbf{V}^* \cdot \nabla^* \mathbf{V}^* = -Eu\nabla^* p^* + \frac{1}{\mathrm{Re}}\nabla^{*2}\mathbf{V}^* + Fr^{-2}\mathbf{f}^* \tag{2}$$

where $\mathbf{V}$ is the velocity vector, $\mathbf{f}$ is the volume force, *St* is the Strouhal number, *Eu* is the Euler number, *Fr* is the Froude number and superscript"*" denotes the variables are dimensionless.

The dimensionless coefficients in the equation (2) are four similarity numbers. Owing to the minor impact of gravity, volume force is neglected here. For similar operating conditions of scaled geometries, *St* and *Eu* are the same. As the dimensionless velocity fields in the distributor of model and prototype turbines are highly close to each other, $\mathbf{V}^*$ is considered approximately identical for the two turbines. Thus, it can derived from the above analysis that:

$$\frac{1}{\mathrm{Re}_m}\nabla_m^{*2}\mathbf{V}_m^* - Eu\nabla_m^* p_m^* \approx \frac{1}{\mathrm{Re}_p}\nabla_p^{*2}\mathbf{V}_p^* - Eu\nabla_p^* p_p^* \tag{3}$$

where subscripts "*m*" and "*p*" denote model and prototype, respectively. It can be concluded from equation (3) that the larger the Reynolds number, the smaller the pressure gradient. As the prototype possesses larger Reynolds number, its relative amplitude of pressure fluctuation is smaller than that of model turbine. Since the flow patterns and pressure fluctuation characteristics of the two turbines show eminent similarity in the RSI region, it is considered meaningful to predict the RSI condition of prototype turbine based on the model test results.

Downstream the RSI region in the runner, the flow is convectively accelerated with severe separation and the impact of Reynolds number becomes prominent, showing discrepancy of flow patterns in the runner, as shown in figure 8 and figure 10. It can be seen that the flow pattern in the model turbine is more disorganized than that in the prototype one, with evident separation on each suction side of runner blade, while for prototype turbine the flow pattern is quite different with less severe flow separation. The channel vortices of the two turbines are presented in figure 9, showing more vortices in the model turbine compared to the prototype one. In figure 11, the low frequencies of pressure fluctuation with relative amplitude over 0.8% correspond to the channel vortex motion in the runner, which is 0.676fn for the model turbine and 0.696fn for the prototype turbine, while with relative amplitude lower than 0.4% correspond to vortex rope motion downstream the runner which will be discussed in the next section. The guide vane passing frequency, 20fn, is identical for the two turbines due to the guarantee of Strouhal number equivalence. It seems that similarity of both flow patterns and pressure fluctuation substantially fades in the runner due to different topological structure of flow separation and vortex formation dependent on different Reynolds numbers.

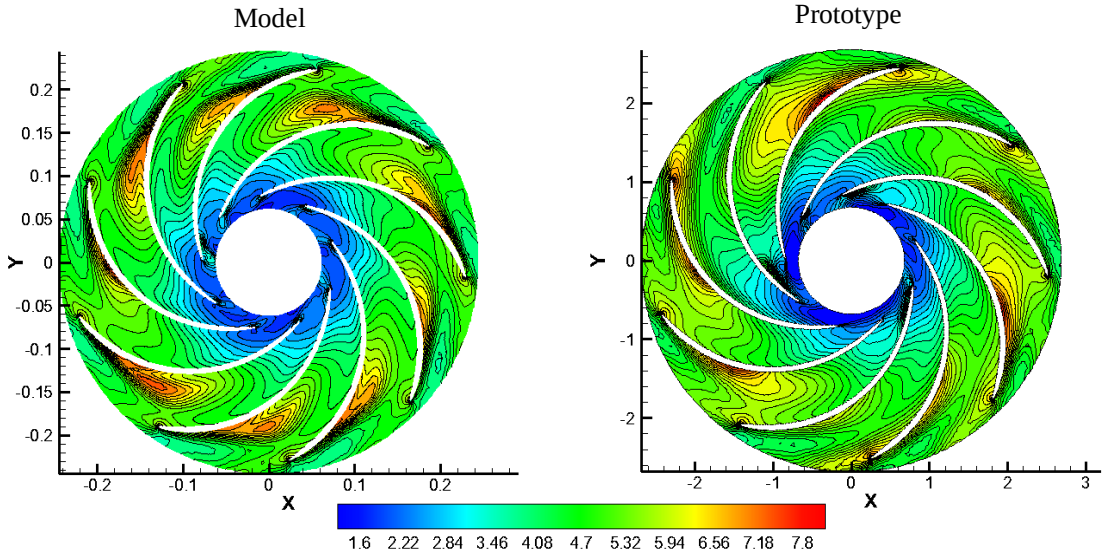

Figure 8. Comparison of dimensionless velocity field at mid-height of the runner

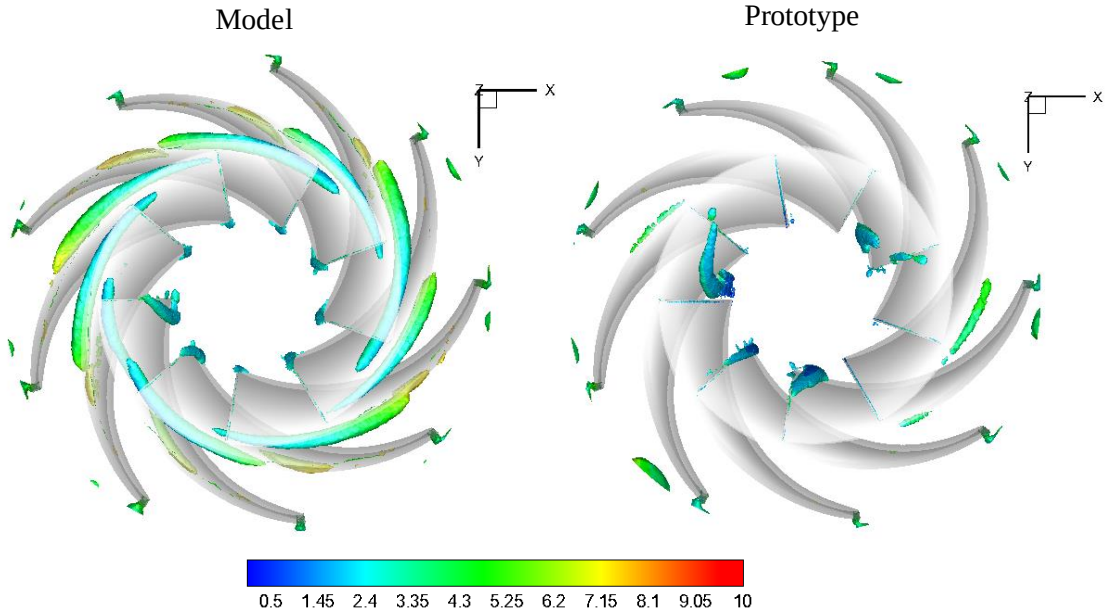

Figure 9. Comparison of isosurface Q*=800 in the runner(coloured by dimensionless velocity)

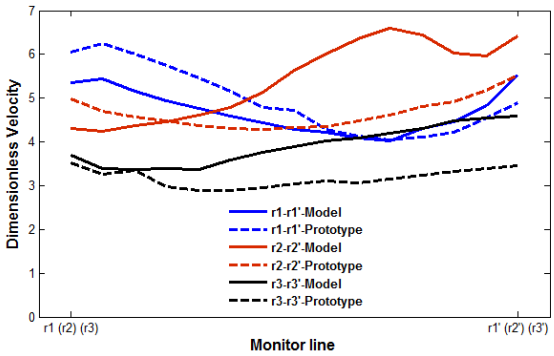

Figure 10. Dimensionless velocity at monitor lines r1-r1', r2-r2' and r3-r3' in the runner

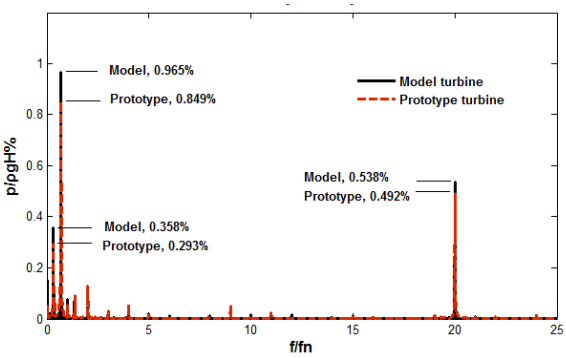

Figure 11. Pressure fluctuation spectrum at monitor point P2

3.3. Flow Pattern and Pressure Fluctuation of partial discharge condition in the Draft Tube

In the draft tube where the flow is diffusively decelerated, similarity is debilitated owing to different vortex rope formation impacted by the prominent effect of Reynolds number. As shown in figure 12, the vortex rope in model turbine extends to the diffusion section of the draft tube, while in prototype turbine it ends in the middle of the elbow section presenting in different size and shape. Figure 13 highlights the dimensionless tangential velocity (defined as $V_\theta^* = V_\theta / V_{inlet}$) at three monitor lines in the draft tube cone. It is noted that the dimensionless tangential velocity of prototype turbine is smaller than that of model turbine indicating a slower circumferential motion of vortex rope, which corresponds to a smaller low frequency of pressure fluctuation, as shown in figure 14. The low frequency in the draft tube for model turbine is 0.323fn, while for prototype turbine it is 0.305fn. It can be also observed that the relative pressure fluctuation amplitude of prototype turbine is smaller than that of model one.

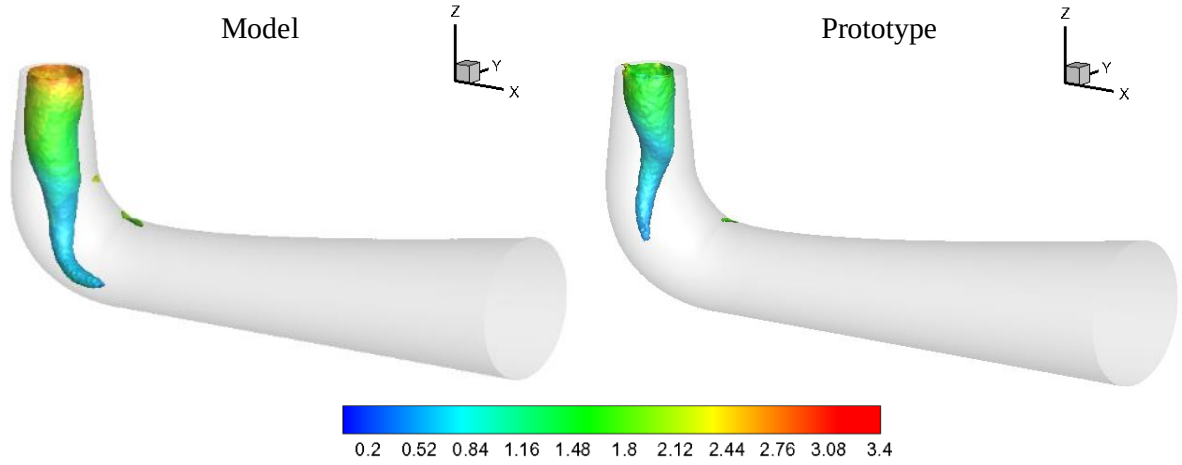

Figure 12. Comparison of isosurface $p^* = -0.045$ in the draft tube (coloured by dimensionless velocity)

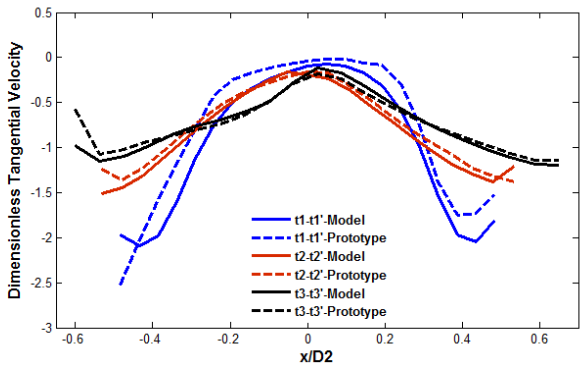

Figure 13. Dimensionless tangential velocity at monitor lines t1-t1', t2-t2' and t3-t3' in the draft tube

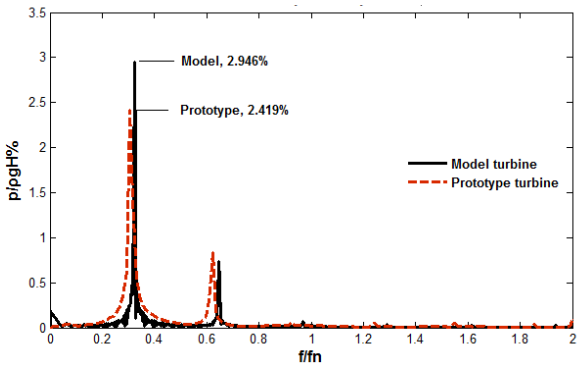

Figure 14. Pressure fluctuation spectrum at monitor point P3 in the draft tube

With the assumption of $V_r \approx 0$ and $\partial V_\theta / \partial \theta \approx 0$, the dimensionless Navier-Stokes equation of cylindrical coordinate system in *r* direction can be simplified as:

$$\frac{V_\theta^{*2}}{r^*} = Eu \frac{\partial p^*}{\partial r^*} \tag{4}$$

Thus it can be concluded from equation (4) that the larger the tangential velocity, the larger the pressure gradient, which results in larger pressure fluctuation in the draft tube. As the dimensionless

tangential velocity in model turbine is larger, the amplitude of pressure fluctuation in model turbine draft tube is greater accordingly. The theoretical analysis is in accordance with the simulation results presented in figure 14.

4. Conclusion

Failing to guarantee the equivalence in Reynolds number of model and prototype brings about discrepancy in external characteristics, inner flow pattern and pressure fluctuation. The current paper focuses on the similarity study of model turbine and prototype and the impact of Reynolds number on their performance differences in partial discharge condition.

1. In the RSI region where Strouhal number plays a leading role, the flow is convectively accelerated with minor flow separation, contributing to a high level of similarity in flow pattern. The characteristic frequencies of pressure fluctuation are identical for the two turbines while the pressure fluctuation amplitude of model turbine is slightly higher than that of prototype turbine. Thus, it can be concluded that similarity of flow pattern and pressure fluctuation occurs in the RSI region. For the prediction of flow pattern and pressure fluctuation caused by RSI, model test results can provide a good reference to prototype operation.
2. Downstream the RSI region in the runner where the flow is convectively accelerated with severe separation, similarity substantially fades due to different topological structure of flow separation and vortex formation dependent on distinctive Reynolds numbers.
3. In the draft tube where the flow is diffusively decelerated, similarity becomes debilitated owing to different vortex rope formation impacted by the prominent effect of Reynolds number. The relative amplitude and characteristic frequency of pressure fluctuation in model turbine are both larger than those of prototype turbine.

The above analysis and conclusion are drawn based on numerical simulation on pumped turbines without consideration of penstock response and resonance. In fact, the conclusions may be different when model test results are compared with field measurements. The pressure fluctuation instability in the draft tube of prototype turbine under real operation condition can be much more significant [1] [3] for three factors: (1) Dissimilarities of boundary conditions occurs in model and prototype test conditions. For instance, the interference of penstock in prototype turbine can be huge, which may result in greater pressure fluctuation. However, those are not considered in the simulation; (2) Resonance is more likely to happen in prototype turbine circumstances; (3) Difference in Froude number of the two turbines may carry out scale effects on the vortex rope cavity volume, however, in the current simulation gravity is not part of the scope. Our future work will focus on the effects of these factors in producing discrepancies in model and prototype turbines.

Acknowledgments

The authors takes this opportunity to thank the National Science and Technology Ministry of China and Harbin Electric Machinery Company Limited (ID: 2011BAF03B01-02) for their financial support.

References

[1] Bue I L. Pressure pulsations and stress in a high head turbine: comparison between model and geometrically similar prototype. *Master disseration*, Norwegian University of Science and Technology, Trondheim, Norway, 2013, **4**, 33

[2] Jacob T, Prénat J, Vullioud G and Araguas B L. Surging of 140MW Francis turbines at high load, analysis and solution. *Proceedings of 16th IAHR Symposium on Hydraulic Machinery and Systems (Sao Paolo, Brazil)*, 1992

[3] Alligné S, Maruzewski P, Dinh T, Wang B, Fedorov A, Iosfin J and Avellan F. Prediction of a Francis turbine prototype full load instability from investigations on the reduced scale model. *Proceedings of 25th IAHR Symposium on Hydraulic Machinery and Systems (Timisoara, Romania), IOP Conference Series: Earth and Environmental Science*. IOP Publishing, 2010, 12(1) 012025

[4] Wu Y L, Liu S H, Dou H S, et al. Numerical prediction and similarity study of pressure fluctuation in a prototype Kaplan turbine and the model turbine. *Computers & Fluids*, 2012, **56** 128-142
[5] Liu S H, Mai J Q, Shao J and Wu Y L. Pressure pulsation prediction by 3D turbulent unsteady flow simulation through whole flow passage of Kaplan turbine. *Engineering Computations*, 2009, **26**(8) 1006-1025
[6] Schewe G. Reynolds-number effects in flow around more-or-less bluff bodies. *Journal of Wind Engineering and Industrial Aerodynamics*, 2001, **89**(14) 1267-1289
[7] Schewe G. Reynolds-number-effects in flow around a rectangular cylinder with aspect ratio 1: 5. *Journal of Fluids and Structures*, 2013, **39** 15-26
[8] Mannini C, Šoda A and Schewe G. Unsteady RANS modelling of flow past a rectangular cylinder: Investigation of Reynolds number effects. *Computers & Fluids*, 2010, **39**(9) 1609-1624
[9] Yan J, Koutnik J, Seidel U and Huebner B. Compressible simulation of rotor-stator interaction in pump-turbines. *Proceedings of 25th IAHR Symposium on Hydraulic Machinery and Systems (Timisoara,* Romania), *IOP Conference Series: Earth and Environmental Science*. IOP Publishing, 2010, **12**(1) 012008